



# **COMPUTATIONAL STUDY OF ISING MODEL AND IT'S APPLICATION IN OPTIMIZATION USING QUANTUM ANNEALING**



**A PROJECT WORK REPORT  
SUBMITTED TO THE DEPARTMENT OF PHYSICS  
TRI-CHANDRA MULTIPLE CAMPUS  
TRIBHUVAN UNIVERSITY**

**IN THE PARTIAL FULFILLMENT OF THE REQUIREMENTS  
FOR THE AWARD OF THE DEGREE OF  
BACHELOR OF SCIENCE IN PHYSICS**

**By**

**HARI RAM KRISHNA GAULI  
TU REG. NO.: 5 - 2 - 37 - 321 - 2016  
SYMBOL NO.: 371246**

**UNDER THE ESTEEMED GUIDANCE OF  
ASST. PROF. KARAN GIRI AND  
DR. DIBAKAR SIGDEL**

**March, 2021**



## DECLARATION

Project report entitled “**COMPUTATIONAL STUDY OF ISING MODEL AND IT’S APPLICATION IN OPTIMIZATION USING QUANTUM ANNEALING**” which is being submitted to the Department of Physics, Tri-Chandra Multiple Campus; is a project work carried out by me under the supervision of Asst. Prof. Karan Giri and Dr. Dibakar Sigdel.

I hereby declare that this written submission represents my ideas in my own words and where other’s ideas or words have been included; I have cited the references of the original sources that I have used.

Mr. Hari Ram Krishna Gauli  
B.Sc. 4<sup>th</sup> year  
TU Reg no.: 5 - 2 - 37 - 321 - 2016  
Symbol no.: 371246  
Department of Physics  
Tri-Chandra Multiple Campus  
Ghantaghar, Kathmandu, Nepal

Date:.....



## RECOMMENDATION

It is certified that **Mr. Hari Ram Krishna Gauli** has carried out this project work entitled **“COMPUTATIONAL STUDY OF ISING MODEL AND IT’S APPLICATION IN OPTIMIZATION USING QUANTUM ANNEALING”** under our supervision. He has fulfilled all the requirement laid down by the Institute of Science and Technology (IoST), Tribhuvan University, Kirtipur for the submission of the project work. We recommend the project work in the partial fulfillment for the requirement of Bachelor’s Degree of Science in Physics.

Asst. Prof. Karan Giri  
(Supervisor)  
Tri-Chandra Multiple Campus  
Ghantaghar  
Kathmandu, Nepal

Dr. Dibakar Sigdel  
(Co-supervisor)  
University of California  
Los Angeles  
California, USA



## LETTER OF APPROVAL

We certify that we have read this project work report and in our opinion, it is good in the scope and quality as a project work report in partial fulfillment for the requirement of Bachelor's Degree of Science in Physics.

### Evaluation Committee

\_\_\_\_\_  
Asst. Prof. Karan Giri  
(Supervisor)

\_\_\_\_\_  
Asst. Prof. Iswar Prasad Koirala  
(Head)  
Department of Physics  
Tri-Chandra College, Ghantaghar  
Kathmandu, Nepal

\_\_\_\_\_  
Dr. Dibakar Sigdel  
(Co-supervisor)

\_\_\_\_\_  
External Examiner

\_\_\_\_\_  
Internal Examiner

Date:.....



## CERTIFICATE

This is to certify that, on the recommendation of **Asst. Prof. Karan Giri** and **Dr. Dibakar Sigdel**, this project report submitted by **Mr. Hari Ram Krishna Gauli** entitled “**COMPUTATIONAL STUDY OF ISING MODEL AND IT’S APPLICATION IN OPTIMIZATION USING QUANTUM ANNEALING**” is forwarded by Department of Physics, Tri-Chandra Multiple Campus to the office of the controller of examination, Tribhuwan University, Balkhu.

\_\_\_\_\_  
Asst. Prof. Karan Giri  
(Supervisor)

\_\_\_\_\_  
Asst. Prof. Iswar Prasad Koirala  
(Head)  
Department of Physics  
Tri-Chandra College, Ghantaghar  
Kathmandu, Nepal

\_\_\_\_\_  
Dr. Dibakar Sigdel  
(Co-supervisor)

Date:.....

## ACKNOWLEDGEMENTS

First of all, I would like to express my deep gratitude and sincere respect to supervisors Asst. Prof. Karan Giri and Dr. Dibakar Sigdel for their continuous support to my work. I am deeply indebted to Dr. Dibakar Sigdel for his constant guidance and advice regarding entire work.

Secondly, I present profound thankfulness to Asst. Prof. Iswar Prasad Koirala, Head of the Department of Physics, Tri-Chandra Multiple Campus for his encouragement and suggestion. I thank Asst. Prof. Madhu Sudan Paudel for his guidance to prepare this report in LATEX. My thankfulness is extended to faculty members of the Department for their suggestions and contribution throughout my Bachelor in Science. I would also like to acknowledge the staffs of administration and library of Tri-Chandra Multiple Campus for their help and cooperation.

Moreover, I am grateful to ANPA team for providing opportunity to carry out project work with expert in topic of my interest. I would also like to mention seniors Mr. Saurav Khadka, Mr. Rahul Nepal, Mr. Saurav Mishra, Ms. Denisha Pantha and my friend Mr. Aayush Gautam for their continuous support regarding the project work.

Finally, I would like to mention my parents for being there to support me in pursuing subject of my interest.

## **ABBREVIATIONS**

**MCMC:** Markov Chain Monte Carlo  
**IM:** Ising Model  
**BM:** Binary Model  
**BQM:** Binary Quadratic Model  
**QUBO:** Quadratic Unconstrained Binary Optimization  
**PBC:** Periodic Boundary Condition  
**FBC:**Free End Boundary condition  
**CO:** Combinatorial Optimization  
**AQC:** Adiabatic Quantum Computation  
**EBM:** Energy Based Model  
**QPU:** Quantum Processing Unit  
**QA:** Quantum Annealing  
**NP:** Non-deterministic Polynomial Time  
**SWE:** Schrodinger's Wave Equation  
**TSP:** Traveling Salesman Problem  
**MVC:** Minimum Vertex Cover  
**CSP:** Constraint Satisfaction Problem



## ABSTRACT

In this project work, Markov Chain-Monte Carlo simulation technique was used to study the phase transition in two dimensional Ising Model in a square lattice. The study of temperature dependence of average magnetization and specific heat in different magnetic field has been carried out in  $3 \times 3$  lattice with periodic boundary. The simulation was done in three dimensional  $3 \times 3 \times 3$  lattice as well. The simulation in 2D was then transformed into binary variant and QUBO formulation was used to solve the problem. The simulation for binary variant has been done using dimod package in Python as a programming language. Critical temperature points  $k_B T_c / J$  of 2D and 3D IM has been observed at about 2.2 and 4.3 respectively. The simulation suggests bifurcation in average magnetization below critical temperature  $T_c$ . We found IM exhibits interesting features like spontaneous magnetization and symmetry breaking below  $T_c$ . The temperature necessary for disorderness increases for higher field  $B$ , showing contribution of external field. This work also explores application of quantum annealing to solve combinatorial optimization problems using QUBO approach.

# Contents

<b>DECLARATION</b>	<b>i</b>
<b>RECOMMENDATION</b>	<b>ii</b>
<b>EVALUATION</b>	<b>iii</b>
<b>CERTIFICATE</b>	<b>iv</b>
<b>ACKNOWLEDGEMENTS</b>	<b>v</b>
<b>ABBREVIATIONS</b>	<b>vi</b>
<b>ABSTRACT</b>	<b>vii</b>
<b>1 Introduction</b>	<b>1</b>
1.1 Background . . . . .	1
1.2 Motivation . . . . .	2
1.3 Objective . . . . .	2
<b>2 Literature Review</b>	<b>3</b>
<b>3 Theory</b>	<b>5</b>
3.1 Partition Function . . . . .	5
3.2 Boltzmann Probability . . . . .	5
3.3 Relative Probability . . . . .	5
3.4 Thermodynamic Quantities of Interest . . . . .	6
3.5 Ising Model in One Dimension . . . . .	6
3.5.1 Hamiltonian of 1D IM . . . . .	6
3.5.2 Partition Function in 1D IM . . . . .	7
3.5.3 Combinatorial Approach Towards 1D IM without Interaction i.e. $J=0$ . . .	10
3.5.4 Neighboring Interaction at zero external field in 1D IM i.e. $B=0$ . . . . .	11
3.6 IM in 2D . . . . .	12
3.6.1 Combinatorial Approach Towards solving 2D IM at Zero Field . . . . .	12
3.7 Markov Chain Monte Carlo Simulation . . . . .	14
3.8 Quantum Computing . . . . .	15
3.8.1 Adiabatic Quantum Computation . . . . .	15

3.8.2	Quantum Annealing . . . . .	16
3.8.3	Combinatorial Optimization Problems . . . . .	17
3.8.4	Quadratic Unconstrained Binary Optimization . . . . .	17
3.8.5	D-WAVE Hardware : QPU . . . . .	17
3.8.6	Minor Embedding . . . . .	18
<b>4</b>	<b>Method of Analysis</b>	<b>19</b>
4.1	2D BM in a finite lattice . . . . .	19
4.2	Network Graph . . . . .	19
4.3	Binary Quadratic Model . . . . .	20
4.4	Interaction in Binary Quadratic Model . . . . .	20
4.4.1	Neighboring Interaction in BM . . . . .	21
4.4.2	Self Energy in BM . . . . .	22
4.5	Hamiltonian for Binary Model . . . . .	22
4.6	QUBO Formulation of IM . . . . .	22
4.7	Markov Chain . . . . .	23
4.8	Simulation Scheme . . . . .	23
4.9	Metropolis Algorithm . . . . .	23
4.10	CO Problems . . . . .	24
4.10.1	The Number Partitioning Problem . . . . .	24
4.10.2	Map Coloring Problem . . . . .	25
4.10.3	Minimum Vertex Cover Problem . . . . .	28
<b>5</b>	<b>Results and Discussion</b>	<b>31</b>
5.1	Simulation in 2D IM . . . . .	31
5.1.1	Thermalization in 2D IM . . . . .	31
5.1.2	Findings of 2D IM . . . . .	31
5.2	Equivalence with Binary Variant of IM . . . . .	33
5.3	Simulation in 3D IM . . . . .	34
5.3.1	Thermalization in 3D IM . . . . .	35
5.3.2	Findings of 3D IM: . . . . .	35
5.4	Optimal Solution of QUBO Problems . . . . .	37
5.4.1	Number Partitioning Problem . . . . .	37
5.4.2	Map Coloring Problem . . . . .	37
5.4.3	Minimum Vertex Cover Problem . . . . .	38
<b>6</b>	<b>Conclusion and Future Work</b>	<b>39</b>
6.1	Conclusion . . . . .	39
6.2	Future Work . . . . .	39
	<b>References</b>	<b>41</b>
	<b>AppendixA</b>	<b>43</b>
<b>A</b>	<b>Documentation of Codes</b>	<b>43</b>

# Chapter 1

## Introduction

### 1.1 Background

Ising Model was a problem given by Wilhelm Lenz to his student Ernst Ising for his PhD thesis, which was published in 1925 [1]. It was a simple statistical mechanical model to study phase transition in ferromagnets with one-dimensional chain of spins which are represented by either +1 or -1. Later, in 1943 Onsager [2] solved the two-dimensional IM in zero field, by using transfer matrix technique and group theory. Even nearly after a century, the model remains one among the few analytically solved statistical problem with its applications in wide disciplines of science.

Phase transition is characterised by abrupt change in a physical quantity with small variation of parameter. Ising found no phase transition in one-dimensional IM and concluded the similar expectation for higher dimensions. Onsager found there exists phase transition in two dimensional model. Exact solution of higher dimensional IM has remained intractable problem for both physicists and mathematicians, although various approximation works have been done. In order to address this issue, a powerful algorithm has been developed, called Markov-Chain Monte Carlo simulation, whose results elegantly match with theory.

R.P. Feynman, in 1981, discussed about the possibility of a computer that will do exact simulation same as by nature. It has been theoretically and experimentally proven that nature follows the rules of quantum mechanics at microscopic levels. He added an example of polarization of photon (a two-state system) to make his point that quantum mechanics can't seem to be imitable by a local classical computer [3]. Classical computer uses classical physics which are deterministic in nature while quantum mechanics is probabilistic and is reversible. A quantum computer is a device that leverages certain properties described by quantum mechanics to perform computation. The working mechanism of QCs is based on quantum mechanical properties like entanglement, superposition and reversibility. This gives QCs a certain kind of advantages over classical ones. Different algorithms have been designed to do same task whose equivalence in classical computing performs rather slow and lacks efficiency in performance. Finding optimal solution of combinatorial optimization problem in QC by annealing has been found to be fast which remains time consuming NP hard problem for classical computers.

## 1.2 Motivation

- Ising Model can be transformed into binary variant with spins either 0 or 1, and hence both IM and binary model are mathematically equivalent.
- Combinatorial optimization problems can be solved by designing hamiltonian of the problem and embedding into QPU hardware of annealers like D-WAVE.
- Monte Carlo Simulation is being used in wide varieties of statistical physics problems. It is being used in lattice calculations in field theory as well. Two dimensional IM has paved a path towards computational simplification of non-perturbative field theory.
- Ising Model is now widely recognized as a testing ground for new theories of phase transition. IM being simplest model, all other models should at least exhibit the behaviour shown by IM plus additional features.
- IM has been used in study of protein folding, image re-construction, neural network etc. It has been widely celebrated in various fields.

## 1.3 Objective

Following are the major objectives of this work:

- To simulate phase transition in a finite two dimensional lattice of size  $3 \times 3$  with 9 spins.
- To formulate a binary variant of IM and simulate phase transition using BQM in dimod python package.
- To simulate phase transition in a finite three dimensional lattice of size  $3 \times 3 \times 3$  with 27 spins.
- To find the plot of magnetization and specific heat as a function of temperature obtained from MCMC simulation.
- To compare the simulation results of two-dimensional IM with analytical results.
- To find the critical point of 3D IM and study behavior of phase transition.
- To formulate QUBO form of combinatorial optimization problems and find their optimal solution.

# Chapter 2

## Literature Review

Ising model is a famous toy model of ferromagnetic phase transition whose two dimensional analytic treatment is still under development. It has been subject of successive historical development following the proof of existence of phase transition in 2D by Peierls [4], the prediction of critical temperature by Kramers and Wannier [5], and computation of its free energy by Onsager [2]. There are thousands of paper on the subject but celebrated gateway to recent developments in IM is a classical text of McCoy and Wu [6]. There are variety of approaches to understand analytical solution of two dimensional Ising Model in zero field. We will focus on the easiest one, i.e. combinatorial approach which is mathematically less rigorous and this approach includes a series of historical works. Our problem will reduce into counting number of closed loops in a graph by this approach [7,8].

Metropolis [9] explained the standard method of drawing sample configuration of IM for particular temperature from random configuration of phase space. The method employs making use of Markov Chain to generate desired sample. The key idea is to construct a transition probability for the Markov chain such that it has a Boltzmann distribution. K. Binder [10] discussed application of Monte-Carlo method to problems of statistical physics.

T.D. Lee and C. N. Yang [11] used 0s and 1s to represent lattice sites in lattice-gas model. They proved problems of an Ising model in a magnetic field and a lattice gas are mathematically equivalent. The literature on QUBO goes back to the 1968 where the topics of pseudo-boolean functions and binary quadratic optimization were introduced by Hammer and Rudeanu [12]. Boros and Hammer [13] discuss the use of QUBO as an approach for modeling the Max-Cut problem. Their paper highlights the relationship between QUBO, Max-cut, Max 2-sat, and the Weighted Signed Graph problem. Pardalos and Xue [14] discussed the relationship between the maximum clique problem, the maximum independent set problem, and the vertex cover problem, indicating how each can be represented by QUBO.

Pardalos and Du [15] discuss the maximum clique problem and how it can be modeled in a variety of ways including a representation in terms of QUBO. The authors provide a very broad and in depth discussion of a variety of applications and of both exact and heuristic solution methods for

the MC problem. Computational experience with various solution approaches to the MC problem is also presented.

Alidaee, Glover, Kochenberger, and Rego [16] discuss the number partitioning problem where the objective is to assign numbers to subsets such that the sums of the numbers in each subset are as close as possible to one another. The authors show that the  $n = 2$  subset case can be modeled as an instance of QUBO and that problems with  $n > 2$  can be modeled as a constrained version of QUBO. Extensions of the basic model along with computational experience for the  $n=2$  case are presented indicating the attractiveness of the approach.

Optimization of binary variables has been a great application area of recent quantum hardware developments based on annealing like DWAVE. Quantum Computation is an active research field due to its capability to outperform classical computer. The term quantum annealing first appeared in [17,18] where, the authors used quantum transition for state search. Quantum annealing in the present sense using natural Schrodinger dynamics was proposed later independently in [19] and [20]. In paper [21], the mathematical proof of convergence of results of QA to that of simulated Monte-Carlo annealing has been discussed. QA has been discussed as new method of finding extrema of multidimensional function to avoid local minima and find global minima in [19].

Quantum computation offers many new and exciting capabilities to science, technology and humanity. Every combinatorial optimization problem has revealed its simplification using QUBO technique, which is then feed as input to annealer. The speed advantage over classical computer is so significant that many researchers believe that no conceivable amount of progress in classical computer would be able to overcome the gap between the power of a classical computer and the power of a quantum computer [33] . In order to formulate QUBO problem, we will start with graph of nodes and edges and assign bias to each node, coupler to each edge and a offset [22].

# Chapter 3

## Theory

### 3.1 Partition Function

Partition function is a functional in statistical mechanics under which certain operations are done to get value of physical observable. In other words, partition function contains all the information needed to recover the macroscopic properties of a thermodynamic system with fixed number of particles immersed in a heatbath [24,25]. We will use the expression of partition function without detail formulation of canonical ensemble.

$$\mathcal{Z} = \sum_i e^{-\beta H_i} ; \beta = \frac{1}{k_B T} \quad (3.1)$$

where,

$k_B$ =Boltzmann Constant

$T$ =Absolute Temperature

$i$ =Possible Spin Configuration

$H_i$ =Hamiltonian of state  $i$

### 3.2 Boltzmann Probability

The probability of spin configuration  $i$  is denoted by  $p_i$  which explicitly depends on Hamiltonian  $H_i$  and inverse temperature  $\beta$ .

$$p_i = \frac{e^{-\beta H_i}}{\sum_i e^{-\beta H_i}} = \frac{e^{-\beta H_i}}{\mathcal{Z}} \quad (3.2)$$

Partition function appears as a normalizing factor to ensure probability sum to one in Boltzmann probability.

### 3.3 Relative Probability

Relative probability  $R$  is the ratio of Boltzmann probability of final state  $p_{final}$  to initial state  $p_{initial}$  in a transition.



$$R = \frac{p_{final}}{p_{initial}} = \frac{e^{-\beta H_{final}}}{e^{-\beta H_{initial}}} = e^{-\beta \Delta H} \quad (3.3)$$

where;

$\Delta H = H_{final} - H_{initial} = \text{Change in Hamiltonian}$

### 3.4 Thermodynamic Quantities of Interest

Magnetization

$$M(N, T, \mu B) = \left\langle \sum_{i=1}^N s_i \right\rangle = k_B T \frac{1}{\mu \mathcal{Z}} \frac{\partial}{\partial B} \mathcal{Z} \quad (3.4)$$

Internal Energy

$$E = -\frac{\partial \ln \mathcal{Z}}{\partial \beta} = -\frac{1}{\mathcal{Z}} \frac{\partial \mathcal{Z}}{\partial \beta} \quad (3.5)$$

Specific Heat

$$C_v = \frac{\partial E}{\partial T} \quad (3.6)$$

### 3.5 Ising Model in One Dimension

Topology of one dimensional IM is a chain of spins represented by either up i.e. +1 or down -1

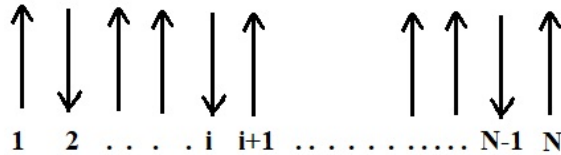


Figure 3.1: 1D IM free end boundary condition

#### 3.5.1 Hamiltonian of 1D IM

Hamiltonian of IM in general depends on external magnetic field B and interaction strength J, where  $\mu$  is moment which represents inherent strength of spins.

$$H = -\mu B \sum_i s_i - J \sum_{i,j} s_i s_j, \text{ where} \quad (3.7)$$

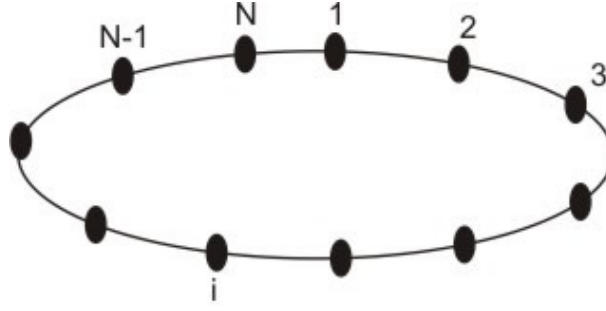


Figure 3.2: 1D IM in periodic boundary condition

$i$  in first term runs over all spins.

$i, j$  in second term runs over non redundant pair of neighboring spins.

First term addresses self energy. For  $B > 0$  first term is negative for  $+1$  spin and positive for  $-1$  spin. This shows up spin i.e.  $+1$  is biased for  $B > 0$ , as it lowers Hamiltonian. Similarly for  $B < 0$ , down spin i.e.  $-1$  is biased.

Second term accounts for interaction between neighbors.  $J > 0$ ; i.e.  $+ve$   $J$  for ferromagnetic substance, assuring same adjacent spins lowers Hamiltonian of system.  $J < 0$  for anti-ferromagnetic substance, favoring opposite spins alignment.

The Hamiltonian for 1D IM in PBC can be written in the form,

$$H = -\mu B \sum_i^N \frac{s_i + s_{i+1}}{2} - J \sum_i^N s_i s_{i+1} = \sum_i^N \left[ -\mu B \frac{s_i + s_{i+1}}{2} - J s_i s_{i+1} \right]$$

$$H = \sum_i^N \mathbf{H}(s_i, s_{i+1}); \text{ where } \mathbf{H}(s_i, s_{i+1}) = -\mu B \frac{s_i + s_{i+1}}{2} - J s_i s_{i+1} \quad (3.8)$$

On examining the value that  $\mathbf{H}(s_i, s_{i+1})$  gives for all possible  $s_i, s_{i+1}$  we get,

$$\mathbf{H}(+1, +1) = -(\mu B + J), \quad \mathbf{H}(+1, -1) = J, \quad \mathbf{H}(-1, +1) = J, \quad \mathbf{H}(-1, -1) = (\mu B - J) \quad (3.9)$$

### 3.5.2 Partition Function in 1D IM

Partition function for 1D IM in PBC reduces to

$$\mathcal{Z} = \sum_{\text{All States}} e^{-\beta H} = \sum_{\text{All States}} e^{-\beta \sum_i^N \mathbf{H}(s_i, s_{i+1})} = \sum_{s=\pm 1} \prod_{i=1}^N e^{-\beta \mathbf{H}(s_i, s_{i+1})} \quad (3.10)$$

$$\begin{aligned}
e^{-\beta \mathbf{H}(+1,+1)} &= e^{\beta(\mu B + J)} \\
e^{-\beta \mathbf{H}(+1,-1)} &= e^{-\beta J} \\
e^{-\beta \mathbf{H}(-1,+1)} &= e^{-\beta J} \\
e^{-\beta \mathbf{H}(-1,-1)} &= e^{-\beta(\mu B - J)} = e^{\beta(J - \mu B)}
\end{aligned}$$

Let us now consider a transfer matrix  $P$ , and denote spin by column matrices  $s_+$  and  $s_-$

$$P \equiv \begin{pmatrix} e^{\beta(J+\mu B)} & e^{-\beta J} \\ e^{-\beta J} & e^{\beta(J-\mu B)} \end{pmatrix} \quad s_+ \equiv \begin{pmatrix} 1 \\ 0 \end{pmatrix} \quad s_- \equiv \begin{pmatrix} 0 \\ 1 \end{pmatrix} \quad (3.11)$$

Then, we can represent the term in equation (3.10) in terms of matrix product representation. i.e

$$e^{-\beta \mathbf{H}(s_i, s_{i+1})} = s_i^T P s_{i+1} \quad (3.12)$$

To illustrate,

$$\begin{aligned}
s_+^T P s_+ &= (1 \ 0) \begin{pmatrix} e^{\beta(J+\mu B)} & e^{-\beta J} \\ e^{-\beta J} & e^{\beta(J-\mu B)} \end{pmatrix} \begin{pmatrix} 1 \\ 0 \end{pmatrix} = e^{\beta(J+\mu B)} \\
s_+^T P s_- &= (1 \ 0) \begin{pmatrix} e^{\beta(J+\mu B)} & e^{-\beta J} \\ e^{-\beta J} & e^{\beta(J-\mu B)} \end{pmatrix} \begin{pmatrix} 0 \\ 1 \end{pmatrix} = e^{-\beta J} \\
s_-^T P s_+ &= (0 \ 1) \begin{pmatrix} e^{\beta(J+\mu B)} & e^{-\beta J} \\ e^{-\beta J} & e^{\beta(J-\mu B)} \end{pmatrix} \begin{pmatrix} 1 \\ 0 \end{pmatrix} = e^{-\beta J} \\
s_-^T P s_- &= (0 \ 1) \begin{pmatrix} e^{\beta(J+\mu B)} & e^{-\beta J} \\ e^{-\beta J} & e^{\beta(J-\mu B)} \end{pmatrix} \begin{pmatrix} 0 \\ 1 \end{pmatrix} = e^{\beta(J-\mu B)}
\end{aligned}$$

Equation (3.10) in matrix form can be written as,

$$\mathcal{Z} = \sum_{s_{\pm}} \prod_{i=1}^N s_i^T P s_{i+1} \quad (3.13)$$

On expanding, we get

$$\mathcal{Z} = \sum_{s_{\pm}} \prod_{i=1}^N s_1^T P s_2 \ s_2^T P s_3 \ s_3^T P s_4 \dots \dots \dots s_{N-1}^T P s_N \ s_N^T P s_1 \quad (3.14)$$

$$\begin{aligned}
\mathcal{Z} &= s_+^T P \left[ \sum_{s_{\pm}} \prod_{i=1}^N s_2 \ s_2^T P s_3 \ s_3^T P s_4 \dots \dots \dots s_{N-1}^T P s_N \ s_N^T P \right] s_+ + \\
& s_-^T P \left[ \sum_{s_{\pm}} \prod_{i=1}^N s_2 \ s_2^T P s_3 \ s_3^T P s_4 \dots \dots \dots s_{N-1}^T P s_N \ s_N^T P \right] s_- \quad (3.15)
\end{aligned}$$

$$\mathcal{Z} = s_+^T P \left[ \sum_{s_{\pm}} \prod_{i=2}^N s_i s_i^T P \right] s_+ + s_-^T P \left[ \sum_{s_{\pm}} \prod_{i=2}^N s_i s_i^T P \right] s_- \quad (3.16)$$

By mathematical induction we can prove the identity

$$\sum_{s_{\pm}} \prod_{i=2}^N s_i s_i^T P = P^{N-1} \quad (3.17)$$

So, the equation (3.16) can be written as,

$$\mathcal{Z} = s_+^T P^N s_+ + s_-^T P^N s_- = \text{Tr}(P^N) \quad (3.18)$$

There exists a unitary matrix  $U$  that diagonalizes every symmetric matrix into  $D$ . Trace remains unchanged after diagonalization.

i.e.  $P = U \cdot D \cdot U^T$  and  $\text{Tr}(P) = \text{Tr}(D)$

The diagonal elements of  $D$  are:

$$\lambda_{\pm} = e^{\beta J} \left[ \cosh \beta \mu B \pm \sqrt{\sinh^2 \beta \mu B + e^{-4\beta J}} \right] \quad (3.19)$$

$P^N$  can hence be written as,

$$P^N = (U \cdot D \cdot U^T) \cdot (U \cdot D \cdot U^T) \cdot \dots \cdot (U \cdot D \cdot U^T) = (U \cdot D^N \cdot U^T) \quad (3.20)$$

$$\text{Tr}(P^N) = \text{Tr}(D^N)$$

$$\begin{aligned} \mathcal{Z} &= \text{Tr}(P^N) = \lambda_+^N + \lambda_-^N \\ &= e^{N\beta J} \left\{ \left[ \cosh \beta \mu B + \sqrt{\sinh^2 \beta \mu B + e^{-4\beta J}} \right]^N \right. \\ &\quad \left. + \left[ \cosh \beta \mu B - \sqrt{\sinh^2 \beta \mu B + e^{-4\beta J}} \right]^N \right\} \end{aligned} \quad (3.21)$$

At zero magnetic field,  $B=0$

$$\begin{aligned}
 \mathcal{Z} &= \text{Tr}(P^N) \\
 &= e^{N\beta J} [(1 + e^{-2\beta J})^N + (1 - e^{-2\beta J})^N] \\
 &= (e^{\beta J} + e^{-\beta J})^N + (e^{\beta J} - e^{-\beta J})^N \\
 &= (2 \cosh \beta J)^N + (2 \sinh \beta J)^N \\
 \mathcal{Z} &= (2 \cosh \beta J)^N [(1 + (\tanh \beta J)^N)]
 \end{aligned} \tag{3.22}$$

At zero interaction strength,  $J=0$

$$\mathcal{Z} = 2^N \cosh^N \beta \mu B \tag{3.23}$$

### 3.5.3 Combinatorial Approach Towards 1D IM without Interaction i.e. $J=0$

If  $n$  spins are up (+1) then, out of total  $N$  spins, number of down spins  $m = N-n$

$$H_i = -\mu B \sum_i s_i = -\mu B(n - m) \tag{3.24}$$

Partition function reduces to

$$\mathcal{Z} = \sum_{\text{All States}} e^{-\beta H} = \sum_{\text{All States}} e^{\beta \mu B \sum_i s_i} \tag{3.25}$$

Arrangement of  $n$  up and  $m$  down spins is a combinatorial problem, with total  $\frac{N!}{n!m!}$  ways.

$$\mathcal{Z} = \sum_{n,m} e^{\beta \mu B(n-m)} = \sum_{n=0}^N \frac{N!}{n!(N-n)!} e^{\beta \mu B(n-m)} \tag{3.26}$$

$$\mathcal{Z} = (e^{\beta \mu B} + e^{-\beta \mu B})^N = 2^N \cosh \beta \mu B \tag{3.27}$$

Average magnetization is given by,

$$M = \frac{1}{N} \sum_{i=1}^N s_i = \frac{(n - m)}{N} \tag{3.28}$$

Average energy is given by,

$$E = (n - m)\mu B \tag{3.29}$$

We can relate average energy and average magnetization,

$$E = \mu M N B \tag{3.30}$$

### 3.5.4 Neighboring Interaction at zero external field in 1D IM i.e. B=0

The Hamiltonian in case of interaction only is,

$$H = -J \sum_{i,j} s_i s_j \quad (3.31)$$

where we sum over two distinct pairs of spin, and these should not be redundant. This can be achieved in 1D Model by taking products of successive spin.

$$H = -J \sum_{i=1}^N s_i s_{i+1} \quad (3.32)$$

Labelling  $p_i = s_i s_{i+1}$ ,

we will have N-1 interacting bonds for free end boundary condition, and flipping every bonds, we get another set of states, so we multiply by 2

$$\mathcal{Z} = \sum_{i=1}^{N-1} e^{-\beta H} = 2 \sum_{i=1}^{N-1} e^{\beta J \sum_i P_i} = 2(2 \cosh \beta \mu B)^{N-1} \quad (3.33)$$

likewise, for periodic boundary in 1D,

$$\mathcal{Z} = (2 \cosh \beta \mu B)^N (1 + \tanh^N \beta \mu B) \quad (3.34)$$

For large number of spins, the 1D Ising Model can be solved analytically, and yields:

$$\frac{E}{J} = -N \tanh \frac{J}{k_B T} \quad (3.35)$$

$$C(K_B T) = \frac{(J/K_B T)^2}{\cosh^2(J/K_B T)} \quad (3.36)$$

$$M(K_B T) = \frac{N e^{\frac{J}{K_B T}} \sinh\left(\frac{B}{K_B T}\right)}{\sqrt{e^{\frac{2J}{K_B T}} \sinh^2\left(\frac{B}{K_B T}\right) + e^{\frac{-2J}{K_B T}}}} \quad (3.37)$$

These equations were originally derived by Plischke and Bergersen [28]. Equation (3.37) clearly precludes 1D IM at B=0 from exhibiting phase transition.

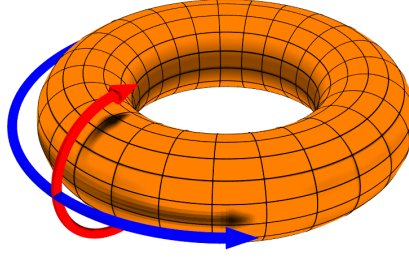


Figure 3.3: Toroidal topology of 2D Ising Model [30] , arrows showing PBC.

## 3.6 IM in 2D

### 3.6.1 Combinatorial Approach Towards solving 2D IM at Zero Field

The partition function of 2D IM at zero field can be written as,

$$\mathcal{Z} = \sum_{\text{All States}} \prod_{\text{Edges } i,j} e^{-\beta J s_i s_j} \quad (3.38)$$

As  $(s_i s_j)^n = 1$  for even  $n$

and  $(s_i s_j)^n = s_i s_j$  for odd  $n$

we can write,  $e^{-\beta J s_i s_j} = \cosh \beta J (1 + s_i s_j \tanh \beta J)$

Since there are  $2N$  bonds for  $N$  lattice sites, equation (3.37) reduces to

$$\mathcal{Z} = \cosh^{2N} \beta J \sum_{\text{All States}} \prod_{\text{Edges } i,j} (1 + w s_i s_j), \text{ where } w = \tanh \beta J \quad (3.39)$$

We can expand

$$\prod_{\text{Edges } i,j} (1 + w s_i s_j) = 1 + w \sum_{i,j} s_i s_j + w^2 \sum_{i_1, j_1} \sum_{i_2, j_2} s_{i_1} s_{j_1} s_{i_2} s_{j_2} + \dots \quad (3.40)$$

Each product terms  $s_i s_j$  in equation (3.39) corresponds to bond formed by neighboring pair of spin. From expansion, we find the consecutive bonds that appear in expansion forming closed graph will only contribute to partition function.

This is due to the fact that  $s$  appearing odd number of times will give zero when summed over  $s = \pm 1$  for all states.

$$\begin{aligned} \sum_{s=\pm 1} s &= 0 \text{ for odd number of } s \text{ spins} \\ \sum_{s=\pm 1} s^2 &= 2 \text{ for even number of } s \text{ spins} \end{aligned} \quad (3.41)$$

Hence, a factor of 2 appears N times for N spins in partition function,

$$\mathcal{Z} = 2^N \cosh^{2N} \beta J [1 + wn(1) + w^2 n(2) + \dots]$$

where  $n(r)$  = number of ways closed graphs formed by r bonds within N lattice sites.

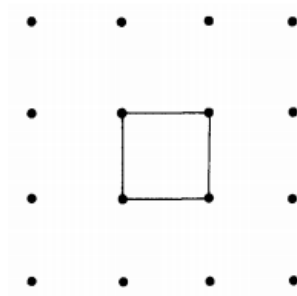


Figure 3.4: Contributing graphs of closed loop of 4 bond

Closed graphs start with number of bonds  $r = 4$ , for which the squares ( Figure 3.4 ) can be placed in N lattice sites. Therefore,  $n(4) = N$ .

There are two possible closed graphs at  $r = 6$  for each lattice site, giving  $n(6) = 2N$  for N sites. The number of closed graphs for higher number of bonds becomes complicated problem which

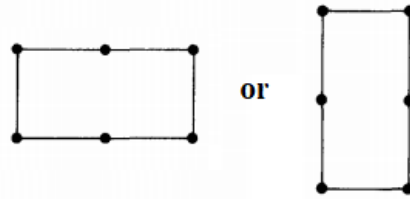


Figure 3.5: Contributing graph of closed loop of 6 bond

has been discussed in text [6].

The partition function will then reduce to

$$\mathcal{Z} = 2^N \cosh^{2N} \beta J [1 + N w^4 + 2N w^6 + \dots] \quad (3.43)$$

Thus the combinatorial graph problem can be solved by finding a generating function  $n(r)$  to find number of ways to form closed graph by r bonds in our lattice.



**Onsager's Results:**

We will only introduce the results of Onsager [2] which we are interested in to compute in MCMC simulation. The magnetization below critical temperature is given by,  
for  $T < T_c$

$$M(T) = \frac{(1 + z^2)^{\frac{1}{4}}(1 - 6z^2 + z^4)}{\sqrt{1 - z^2}} \quad (3.44)$$

$$\text{where } z = e^{\frac{-2J}{k_B T}}$$

for  $T > T_c$   $M(T) = 0$

The critical temperature from theoretical approach is given by relation,

$$k_B T_c = 2.269185 J$$

**3.7 Markov Chain Monte Carlo Simulation**

Monte-Carlo method relies on use of random numbers and helps in probabilistic description of a problem. MCMC which is a sampling technique which leads us to desired phase space configuration corresponding to peak of distribution for a specific temperature. We will start with a random configuration and let the system evolve to a state of uniform energy that maximizes entropy. This process is called thermalization. During the thermalization process, the transition takes place through a sequence of configuration states ; and it produces a Markov Chain . The heart of this algorithm is in generation of a random spin configuration with Boltzmann probability by making decisions to accept or reject random spin flips.

There are some limitations of MCMC method. The computers generate pseudo-random numbers and simulation lacks perfect randomness. It is necessary to take finite lattice size for computation and simulate the system for finite observation time. Statistical Errors arise due to such limitations .

## 3.8 Quantum Computing

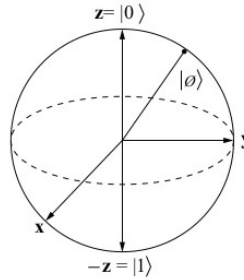


Figure 3.6: The bloch sphere [34].

Classical computers use bits as the basic unit of information. A bit takes one of the two states: 0 or 1. Qubit is similar to the classical bit, however, the main significant difference is that qubits may be in the superposition of both the states  $|0\rangle$  and  $|1\rangle$ . A system described by state vector  $|\Psi\rangle$  is said to be in superposition of state  $|0\rangle$  and  $|1\rangle$  if  $|\Psi\rangle$  is the linear combination of  $|0\rangle$  and  $|1\rangle$ , written as

$$|\Psi\rangle = \alpha |0\rangle + \beta |1\rangle \quad (3.45)$$

where  $\alpha$  and  $\beta$  are complex coefficients called amplitudes of each states following normalization rule:  $|\alpha|^2 + |\beta|^2 = 1$ . A state vector can be visualized as a point on the surface of the three-dimensional unit Bloch sphere shown in Figure 3.6. By convention the north and south poles correspond to the standard basis states  $|0\rangle$  and  $|1\rangle$ , respectively.

A qubit can exist in a continuum of states between  $|0\rangle$  and  $|1\rangle$  - until it is observed. The act of observation affects the state of the system, measurement of the state vector  $|\Psi\rangle$  collapse superposition of the state to one of the two basis states  $|0\rangle$  or  $|1\rangle$ . The square of their amplitude gives the probability of obtaining each state upon measurement. However, direct measurement does not give any information about  $\alpha$  or  $\beta$ . They are obtained by measuring the quantum state of the state vector and other similar state vectors resembling it. The accuracy of measuring  $\alpha$  and  $\beta$  is based on the number of measurements made or numbers of similar quantum states measured. [33,34]

### 3.8.1 Adiabatic Quantum Computation

AQC is an alternative to gate-model of Quantum Computing and is based on evolution of properties of quantum particle according to SWE [34]; given by

$$i\hbar \frac{d}{dt} |\varphi_t\rangle = \mathbf{H}(t) |\varphi_t\rangle \quad (3.46)$$

Here,  $i$  is imaginary unit and  $\hbar = \frac{h}{2\pi}$  where  $h$  is Planck's constant. When time evolves from  $t : 0 \rightarrow t_f$ , we suppose time scale  $s(t) : 0 \rightarrow 1$ .  $H(s)$  be equivalent Hamiltonian during that time and  $\tau(s)$  be rate at which Hamiltonian changes as a function of  $s$ .

$$\frac{d}{ds} |\varphi_s\rangle = -i\tau(s)H(s) |\varphi_s\rangle \quad (3.47)$$

Assuming non degenerate ground state of  $H(s)$ , let  $\delta_m$  denote minimum spectral gap between ground state and excited state at any  $s$ , and provided that  $\tau(s)$  is bounded by

$$\tau_s \gg \left\| \frac{\frac{d}{ds} H(s)}{(\delta_m)^2} \right\| \quad (3.48)$$

Then if  $|\varphi_g\rangle$  be the ground state of the final Hamiltonian, the adiabtic theorem states that,

1. If  $Q$  is in ground state at  $s=0$ , and
2. If  $\delta_m$  is strictly greater than 0 throughout time  $s$ , and
3. If the process evolves slowly enough to obey equation (3.47),

then, the process will finish in ground state  $|\varphi_{tf}\rangle = |\varphi_g\rangle$  with sufficiently high probability.

### 3.8.2 Quantum Annealing

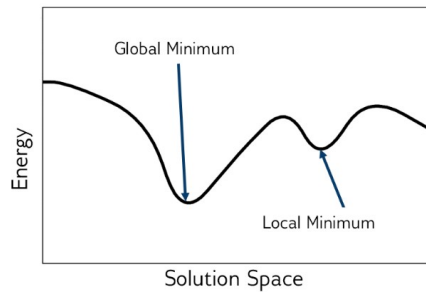


Figure 3.7: Energy of the objective function [23].

Quantum annealing is a heuristic approach to solve problem in combinatorial optimization. QA algorithm is designed to solve a typically NP-hard CO problem, which implies a restriction on the final Hamiltonian of the classical objective function. QA processors naturally return low energy solutions of a CO problem and makes search for best possible combination convenient. It is necessary to formulate objective function for EBM according to CO problem of our interest.

### 3.8.3 Combinatorial Optimization Problems

Combinatorial optimization problems are NP-hard problems, which means they are at least as hard as the hardest problems of NP (non-deterministic polynomial time). The goal of optimization problems is to find a solution to the given problem that either minimizes or maximizes the value of some parameter. It deals with finding optimal combination from a finite set of objects. An algorithm should be implemented in order to solve optimization problem in computer. Once it is known that an algorithm finds a feasible solution, it is necessary to determine whether it has found an optimal solution.

The efficiency of an algorithm depends on time taken by computer to solve the problem and amount of computer memory required to implement the algorithm provided specified size of input value. Computer scientists divide the computational complexity of an algorithm into time complexity and space complexity. The time required to solve a problem depends not only on number of operations that algorithm uses, but also the hardware and software used to run the program. [32]

### 3.8.4 Quadratic Unconstrained Binary Optimization

Combinatorial optimization problems can be reduced to QUBO model and approximately solved by quantum computer in significantly less time compared to classical algorithm. Quantum computing takes advantage of quantum features like superposition, entanglement, reversibility etc. to do so.

QUBO is a NP hard problem, where the objective is to minimize a quadratic polynomial over binary variables. The QUBO model is expressed by the optimization problem given by,

$$\text{minimize/maximize } y = x^T Q x \quad (3.49)$$

where,  $x$  is a vector of binary decision variables and  $Q$  is a square matrix of constants.  $Q$  can be expressed either in symmetric form or upper triangular form. Some examples of QUBO problems include TSP, MVC, Max-Cut Problems etc.

### 3.8.5 D-WAVE Hardware : QPU

The qubits are made from ring of superconducting Niobium, interrupted and controlled by two Josephson junctions maintained below 15mK, and bias represented by  $\phi$  values. Current can flow clockwise, counter-clockwise or in both direction at once when the qubit is in quantum superposition. Couplers form the interconnection between pairs of qubits according to the topology of QPU.

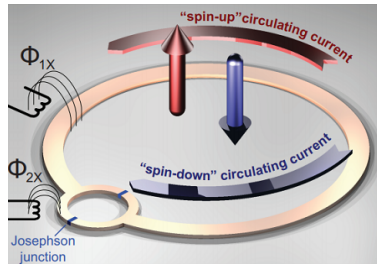


Figure 3.8: Superconducting flux qubit [34].

### 3.8.6 Minor Embedding

The logical qubits should be mapped to physical qubits of quantum computer hardware in order to solve CO problems. Figure 3.10 shows embedding a simple graph into chimera topology QPU of D-WAVE. Embedding is done by adding necessary qubits chains as shown below.

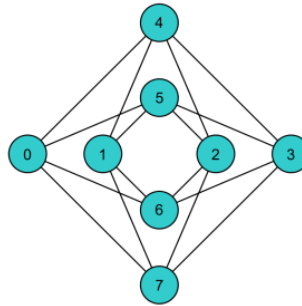


Figure 3.9: Unit cell of qubit in chimera topology [23].

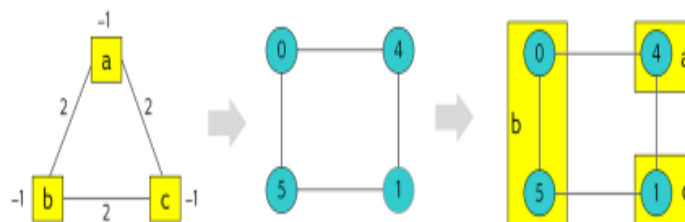


Figure 3.10: Embedding triangular graph [23].

# Chapter 4

## Method of Analysis

### 4.1 2D BM in a finite lattice

For a square lattice consisting  $N$  spins, there are  $\sqrt{N}$  spins in each row, and  $\sqrt{N}$  spins in each column. So, we get total  $N$  vertical edges and  $N$  horizontal edges, giving an aggregate of  $2N$  distinct edges in PBC.

We will consider nine spins in PBC in a  $3 \times 3$  square lattice for our simulation work. Every spin is assigned a scalar value 0 or 1 in Binary Model. Likewise, +1 or -1 in IM.

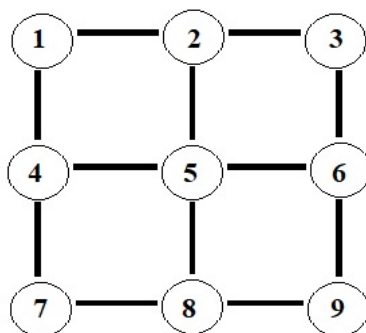


Figure 4.1: 2 D IM in  $3 \times 3$  lattice, periodic links are not shown.

### 4.2 Network Graph

There are nine nodes, each of which are connected to four neighboring nodes in 2D Model with PBC. The set of edges has element  $ij$  which represents edge formed by lattice site labelled  $s_i$  and  $s_j$  is,

Edges= $\{ 12, 13, 14, 17, 23, 28, 25, 36, 39, 45, 46, 47, 56, 58, 69, 78, 79, 89 \}$

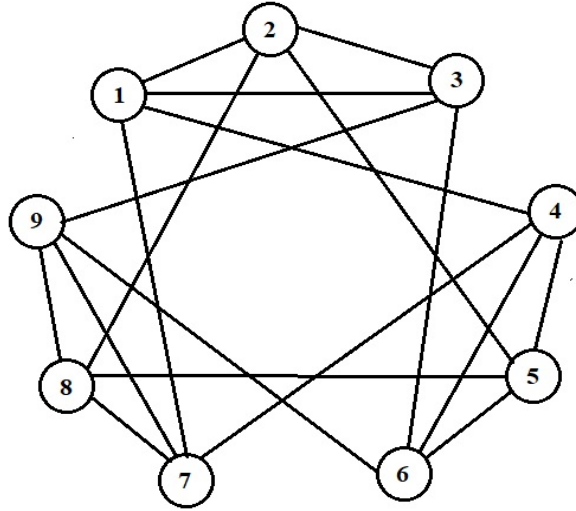


Figure 4.2: Nodes and edges in graph.

### 4.3 Binary Quadratic Model

A binary quadratic model (BQM) is a problem comprising a collection of binary-valued variables (variables that can be assigned two values, for example -1, 1) with associated linear and quadratic biases. We will use 0s and 1s to represent spin instead of +1 and -1. In binary representation of spin,  $s_i^v = s_i$  for  $s_i = 0, 1$ . As a result, higher power terms in spin  $s_i$  will actually be assimilated into linear term.

### 4.4 Interaction in Binary Quadratic Model

The ferromagnetic model favored same identical spins. In binary variant, we will find an expression for Hamiltonian using 0s and 1s. We suppose like spins get lower score 0 and unlike spins get higher score 1. Table 4.1 shows BQM to account interaction in which we give a penalty of higher energy score 1 for interaction with unlike spins and lower score 0 for interaction with like spins.

$s_i$	$s_j$	Interaction	Energy Score
0	0	favors	0
0	1	doesn't favor	1
1	0	doesn't favor	1
1	1	favors	0

Table 4.1: Neighboring interaction of ferromagnetic spins in BM

#### 4.4.1 Neighboring Interaction in BM

We will use a binary quadratic equation to design Hamiltonian for binary variant. In order to find the values of coefficients of equation (4.1), we will plug energy score and spins shown in Table 4.1 and solve the resulting equations.

$$E_{interaction\ score} = a_i s_i + a_j s_j + b_{ij} s_i s_j + C \quad (4.1)$$

For  $s_i = 0, s_j = 0$

$$0 = a_i \cdot 0 + a_j \cdot 0 + b_{ij} \cdot 0 \cdot 0 + C \text{ gives } C = 0$$

For  $s_i = 0, s_j = 1$

$$1 = a_i \cdot 0 + a_j \cdot 1 + b_{ij} \cdot 0 \cdot 1 + 0 \text{ gives } a_j = 1$$

For  $s_i = 1, s_j = 0$

$$1 = a_i \cdot 1 + a_j \cdot 0 + b_{ij} \cdot 1 \cdot 0 + 0 \text{ gives } a_i = 1$$

For  $s_i = 1, s_j = 1$

$$0 = 1 \cdot 1 + 1 \cdot 1 + b_{ij} \cdot 1 \cdot 1 + 0 \text{ gives } b_{ij} = -2$$

Hence, we will get the equation that governs interaction in BM,

$$E_{interaction\ score} = s_i + s_j - 2s_i s_j \quad (4.2)$$

18 edges in network graph are summed over to find  $H_{interaction}$  of a state.

$$H_{interaction} = u \sum_{Edges\ i,j} (s_i + s_j - 2s_i s_j) \quad (4.3)$$

Here,  $u$  characterizes coupling term.



### 4.4.2 Self Energy in BM

In order to bias a particular spin representation, (say 1); we introduce a bias  $v$  so  $-ve v$  will lower energy with a possible constant term  $w$ .

$$H_{self} = v \sum_{node=1}^N (s_{node} + w) \quad (4.4)$$

## 4.5 Hamiltonian for Binary Model

$$\begin{aligned} H_{binary} &= H_{interaction} + H_{self} = u \sum_{Edges\ i,j} (s_i + s_j - 2s_i s_j) + v \sum_{node=1}^N (s_{node} + w) \\ &= u \sum_{Edges\ i,j}^{2N} (s_i + s_j - 2s_i s_j) + v \sum_{node=1}^N s_{node} + Nv w; \text{ where } Nv w \text{ is a constant term} \end{aligned} \quad (4.5)$$

We will use QUBO technique to find Hamiltonian of a state in binary model.

## 4.6 QUBO Formulation of IM

QUBO technique is based on finding upper triangular matrix  $P$  with the help of edges and nodes in network graph. We will first construct a  $N \times N$  matrix and give weights to diagonal elements and elements above it one by one. [22]

In case of nine spins in  $3 \times 3$  lattice, if we represent configuration state of spin by matrix  $U$  as:  $U = (s_1 \ s_2 \ s_3 \ s_4 \ s_5 \ s_6 \ s_7 \ s_8 \ s_9)^T$ , then our matrix to compute Hamiltonian will be,

$$P = \begin{pmatrix} v+4u & -2u & -2u & -2u & 0 & 0 & -2u & 0 & 0 \\ 0 & v+4u & -2u & 0 & -2u & 0 & 0 & -2u & 0 \\ 0 & 0 & v+4u & 0 & 0 & -2u & 0 & 0 & -2u \\ 0 & 0 & 0 & v+4u & -2u & -2u & -2u & 0 & 0 \\ 0 & 0 & 0 & 0 & v+4u & -2u & 0 & -2u & 0 \\ 0 & 0 & 0 & 0 & 0 & v+4u & 0 & 0 & -2u \\ 0 & 0 & 0 & 0 & 0 & 0 & v+4u & -2u & -2u \\ 0 & 0 & 0 & 0 & 0 & 0 & 0 & v+4u & -2u \\ 0 & 0 & 0 & 0 & 0 & 0 & 0 & 0 & v+4u \end{pmatrix}$$

Then, the Hamiltonian can be expressed as,

$$H_{binary} = U^T P U + 9vw \quad (4.6)$$

We will use dimod package in Python to facilitate making this matrix and computing Hamiltonian of arbitrary spin configuration  $U$ .

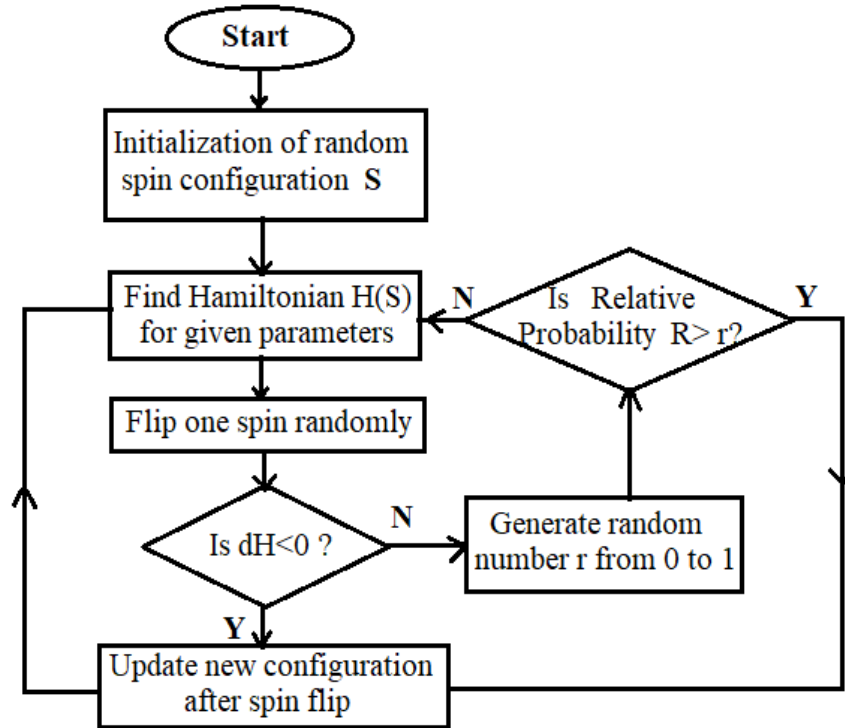


Figure 4.3: MCMC thermalization algorithm.

## 4.7 Markov Chain

Given a finite configuration space, a markov chain is a stochastic process defined by a sequence of random variables such that the probability of being in a particular state at  $(K + 1)^{th}$  step only depends on the state at  $k^{th}$  state.

## 4.8 Simulation Scheme

We will retain history of Hamiltonian and Magnetization during nrun thermalizations which is done at constant temperature. Average of spin, standard deviation of Hamiltonian History and average of Hamiltonian History; only 2000<sup>th</sup> thermalization onwards will be taken for computation of Average Magnetization, Specific Heat and Energy. Then after, we will increase T and repeat the procedure. We have set the values of parameters  $K_b$ , J and  $\mu$  equal to 1 throughout simulation.

## 4.9 Metropolis Algorithm

Thermalization algorithm is implemented in following steps:

1. Starting with arbitrary spin configuration  $U_k = \{s_1, s_2, \dots, s_N\}$
2. Generating a trial configuration  $U_{k+1}$  by picking a random spin  $s_i$  and flipping it  $s_i = 1 - s_i$
3. Calculating Hamiltonian of trial configuration  $H_{trial}$ .  
 If  $H_{trial} \leq H_{S_k}$ , accepting trial by setting  $U_{k+1} = U_{trial}$   
 If  $H_{trial} > H_{S_k}$ , accepting with relative probability  $R = e^{-\Delta E/k_B T}$
4. Choosing uniform random number  $0 \leq r_i \leq 1$   
 Accepting if  $R \geq r_i$  by setting  $U_{k+1} = U_{trial}$   
 Rejecting if  $R < r_i$  i.e.  $U_{k+1} = U_k$

## 4.10 CO Problems

### 4.10.1 The Number Partitioning Problem

Our objective is to partition a set of  $N$  numbers, say  $S = \{4, 5, 7, 9\}$  into two subsets  $S_1$  and  $S_2$  such that subset sums are as close to each other as possible. In order to solve this problem using QUBO approach, we will assign a binary variable  $x_i$  corresponding to each element  $s_i \in S$ .

Let  $x_i=1$  if element  $s_i$  is assigned to set  $S_1$ , and else,  $x_i=0$  if element  $s_i$  is assigned to set  $S_2$ . Then, the sum of elements of set  $S_1$  is given by,

$$sum_1 = \sum_{i=1}^N x_i s_i \quad (4.7)$$

We can get the sum of elements of subset  $S_2$  by subtracting equation (4.7) from total sum  $c = \sum_{i=1}^N s_i$ .

$$sum_2 = \sum_{i=1}^N s_i - \sum_{i=1}^N x_i s_i \quad (4.8)$$

Our motive is to minimize the difference between sum of elements of subsets  $S_1$  and  $S_2$ .

$$\text{difference} = sum_2 - sum_1 = \sum_{i=1}^N s_i - 2 \sum_{i=1}^N x_i s_i = c - 2 \sum_{i=1}^N x_i s_i \quad (4.9)$$

We will square equation (4.9) before formulating a QUBO matrix  $Q$ .

$$\text{difference}^2 = \left[ c - 2 \sum_{i=1}^N x_i s_i \right]^2 = c^2 - 4c \sum_{i=1}^N x_i s_i + 4 \left[ \sum_{i=1}^N x_i s_i \right]^2$$

$$\text{difference}^2 = c^2 - 4c \sum_{i=1}^N x_i s_i + 4 \sum_{i=1}^N (x_i s_i)^2 + 8 \sum_{\text{Edges}=ij} (x_i x_j s_i s_j)$$

Since  $x_i = x_i^2$  for binary variables  $x \in \{0,1\}$ ; we can write,

$$\text{difference}^2 = c^2 + 4 \sum_{i=1}^4 x_i s_i (s_i - c) + 8 \sum_{\text{Edges}=ij} (x_i x_j s_i s_j) \quad (4.10)$$

We see diagonal elements  $q_{ii} = 4s_i(s_i - c)$  and upper diagonal element  $q_{ij} = 8(s_i s_j)$ . In our particular case of  $S=\{4, 5, 7, 9\}$ ,  $N=4$  and total sum  $c=25$ , the nodes and edges in graph of our problem is shown below.

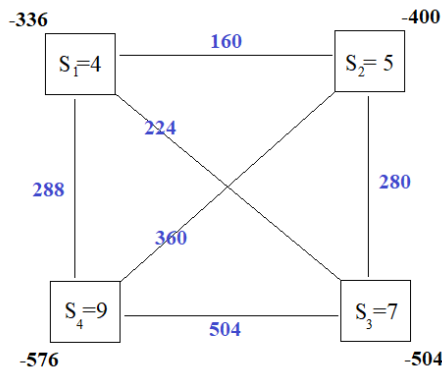


Figure 4.4: Graph showing couplers in at edges and bias in boldface at nodes.

Then, the required upper triangular matrix will be  $Q = \begin{pmatrix} -336 & 160 & 224 & 288 \\ 0 & -400 & 280 & 360 \\ 0 & 0 & -504 & 504 \\ 0 & 0 & 0 & -576 \end{pmatrix}$

The matrix operation that computes our Hamiltonian for particular grouping into two subsets can be expressed as  $c^2 + x^T Q x$  and we are in search of optimal solution  $x^* = (x_1 \ x_2 \ x_3 \ x_4)^T$  which minimizes Hamiltonian. The constant term  $c^2$  in our objective function can be ignored during optimization process.

### 4.10.2 Map Coloring Problem

MCP is a typical constraint satisfaction problem. The objective of this CO problem is to assign a color to each region of a map such that no two adjacent regions have same color. Here, we will try to assign color to each of seven provinces of Nepal in such a way that the adjacent province will have different colors.

Color	Unary Encoding
Red	$q_R, q_G, q_B = 1,0,0$
Green	$q_R, q_G, q_B = 0,1,0$
Blue	$q_R, q_G, q_B = 0,0,1$

Table 4.2: Unary encoding of three colors.

In other words, in case a painter has only 3 colors, the task of assigning color to province so that there will be least number of same colored adjacent province becomes difficult combinatorial optimization problem to solve.

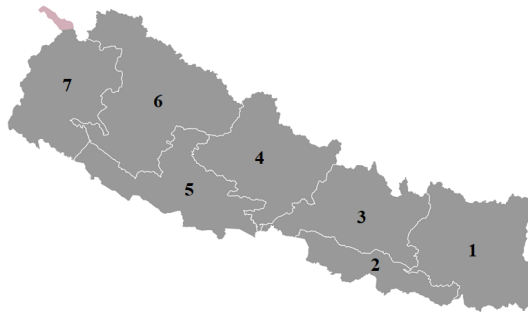


Figure 4.5: Map of Nepal with seven provinces.

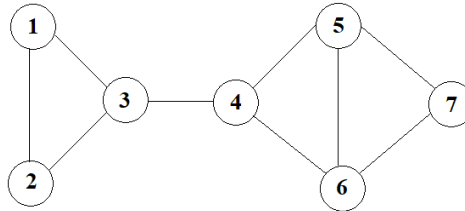


Figure 4.6: Edges connects adjacent provinces labelled by number in nodes of map of Nepal.

There is limit in number of color = 3, let's say we have red , green and blue colors only. Each color can be represented by 3 qubits among which, 1 is for possible color whereas other 2 are zero in unary coding as shown in table below:

Each node represents a province and to assign a color to  $i^{th}$  node requires 3 qubits i.e.  $q_{iR}, q_{iG}, q_{iB}$ . For 7 Provinces, we need 21 binary variables and Q matrix for QUBO formulation will have 21 rows and 21 columns. 21 binary variables are re-labelled here;

$$X = \{q_{1R}, q_{1G}, q_{1B}, q_{2R}, q_{2G}, \dots, q_{7R}, q_{7G}, q_{7B}\} = \{x_1, x_2, x_3, x_4, \dots, x_{19}, x_{20}, x_{21}\}$$

$q_{iR}$ for node i	$q_{jR}$ for node j	Color comparison	Penalty
0	0	both non-red (but could be B-G, G-G)	0
0	1	different	0
1	0	different	0
1	1	same color	1

Table 4.3: Penalty for Color Interaction in MCP.

For valid case,  $q_{iR} + q_{iG} + q_{iB} = 1$  as shown in table above. In order to constrain single color to one province at once, we will introduce a penalty in case of non valid color encoding in every nodes.

$$\begin{aligned}
Penalty_1 &= (q_{iR} + q_{iG} + q_{iB} - 1)^2 \\
&= q_{iR}^2 + q_{iG}^2 + q_{iB}^2 + 2(q_{iR} q_{iG} + q_{iG} q_{iB} + q_{iB} q_{iR}) - 2(q_{iR} + q_{iG} + q_{iB}) + 1 \quad (4.11) \\
&= -(q_{iR} + q_{iG} + q_{iB}) + 2(q_{iR} q_{iG} + q_{iG} q_{iB} + q_{iB} q_{iR}) + 1
\end{aligned}$$

Also, the linked edges should not have same color. In order to formulate Hamiltonian for this issue, for link between nodes i and j, we will check whether same color is assigned to adjacent nodes; and choose higher energy 1 for clear evidence of same color as shown in table.

Now, we will formulate Hamiltonian for later case using BQM given by,

$$Penalty = a_i q_{iR} + a_j q_{jR} + b_{ij} q_{iR} q_{jR} + C$$

$$\text{For } q_{iR} = 0, q_{jR} = 0$$

$$0 = a_i \cdot 0 + a_j \cdot 0 + b_{ij} \cdot 0 \cdot 0 + C \text{ gives } C = 0$$

$$\text{For } q_{iR} = 0, q_{jR} = 1$$

$$0 = a_i \cdot 0 + a_j \cdot 1 + b_{ij} \cdot 0 \cdot 1 + 0 \text{ gives } a_j = 0$$

$$\text{For } q_{iR} = 1, q_{jR} = 0$$

$$0 = a_i \cdot 1 + a_j \cdot 0 + b_{ij} \cdot 1 \cdot 0 + 0 \text{ gives } a_i = 0$$

$$\text{For } q_{iR} = 1, q_{jR} = 1$$

$$1 = 0 \cdot 1 + 0 \cdot 1 + b_{ij} \cdot 1 \cdot 1 + 0 \text{ gives } b_{ij} = 1$$

Hence, we will get the penalty equation for color interaction for later case,

$$Penalty_2 = q_{iR} q_{jR}$$

Similarly , adding penalty due to remaing colors in  $i^{th} - j^{th}$  edge,

$$Penalty_2 = q_{iR} q_{jR} + q_{iG} q_{jG} + q_{iB} q_{jB} \quad (4.12)$$

We add both the penalties and find matrix Q such that total penalty =  $X^T Q X + 21$ . The constant term 21 can be ignored during optimization process. Then, matrix Q can be written as,

$$\begin{bmatrix} -1 & 2 & 2 & 1 & 0 & 0 & 1 & 0 & 0 & 0 & 0 & 0 & 0 & 0 & 0 & 0 & 0 & 0 & 0 & 0 & 0 \\ 0 & -1 & 2 & 0 & 1 & 0 & 0 & 1 & 0 & 0 & 0 & 0 & 0 & 0 & 0 & 0 & 0 & 0 & 0 & 0 & 0 \\ 0 & 0 & -1 & 0 & 0 & 1 & 0 & 0 & 1 & 0 & 0 & 0 & 0 & 0 & 0 & 0 & 0 & 0 & 0 & 0 & 0 \\ 0 & 0 & 0 & -1 & 2 & 2 & 1 & 0 & 0 & 0 & 0 & 0 & 0 & 0 & 0 & 0 & 0 & 0 & 0 & 0 & 0 \\ 0 & 0 & 0 & 0 & -1 & 2 & 0 & 1 & 0 & 0 & 0 & 0 & 0 & 0 & 0 & 0 & 0 & 0 & 0 & 0 & 0 \\ 0 & 0 & 0 & 0 & 0 & -1 & 0 & 0 & 1 & 0 & 0 & 0 & 0 & 0 & 0 & 0 & 0 & 0 & 0 & 0 & 0 \\ 0 & 0 & 0 & 0 & 0 & 0 & -1 & 2 & 2 & 1 & 0 & 0 & 0 & 0 & 0 & 0 & 0 & 0 & 0 & 0 & 0 \\ 0 & 0 & 0 & 0 & 0 & 0 & 0 & -1 & 2 & 0 & 1 & 0 & 0 & 0 & 0 & 0 & 0 & 0 & 0 & 0 & 0 \\ 0 & 0 & 0 & 0 & 0 & 0 & 0 & 0 & -1 & 0 & 0 & 1 & 0 & 0 & 0 & 0 & 0 & 0 & 0 & 0 & 0 \\ 0 & 0 & 0 & 0 & 0 & 0 & 0 & 0 & 0 & -1 & 2 & 2 & 1 & 0 & 0 & 1 & 0 & 0 & 0 & 0 & 0 \\ 0 & 0 & 0 & 0 & 0 & 0 & 0 & 0 & 0 & 0 & -1 & 2 & 0 & 1 & 0 & 0 & 1 & 0 & 0 & 0 & 0 \\ 0 & 0 & 0 & 0 & 0 & 0 & 0 & 0 & 0 & 0 & 0 & -1 & 2 & 0 & 1 & 0 & 0 & 1 & 0 & 0 & 0 \\ 0 & 0 & 0 & 0 & 0 & 0 & 0 & 0 & 0 & 0 & 0 & 0 & -1 & 2 & 0 & 1 & 0 & 0 & 1 & 0 & 0 \\ 0 & 0 & 0 & 0 & 0 & 0 & 0 & 0 & 0 & 0 & 0 & 0 & 0 & -1 & 2 & 2 & 1 & 0 & 0 & 0 & 0 \\ 0 & 0 & 0 & 0 & 0 & 0 & 0 & 0 & 0 & 0 & 0 & 0 & 0 & 0 & -1 & 2 & 0 & 1 & 0 & 0 & 0 \\ 0 & 0 & 0 & 0 & 0 & 0 & 0 & 0 & 0 & 0 & 0 & 0 & 0 & 0 & 0 & -1 & 0 & 0 & 0 & 1 & 0 \\ 0 & 0 & 0 & 0 & 0 & 0 & 0 & 0 & 0 & 0 & 0 & 0 & 0 & 0 & 0 & 0 & -1 & 2 & 2 & 0 & 0 \\ 0 & 0 & 0 & 0 & 0 & 0 & 0 & 0 & 0 & 0 & 0 & 0 & 0 & 0 & 0 & 0 & 0 & -1 & 2 & 0 & 0 \\ 0 & 0 & 0 & 0 & 0 & 0 & 0 & 0 & 0 & 0 & 0 & 0 & 0 & 0 & 0 & 0 & 0 & 0 & -1 & 2 & 0 \\ 0 & 0 & 0 & 0 & 0 & 0 & 0 & 0 & 0 & 0 & 0 & 0 & 0 & 0 & 0 & 0 & 0 & 0 & 0 & -1 & 2 \end{bmatrix}$$

### 4.10.3 Minimum Vertex Cover Problem

The objective of MVC problem is to find set of minimum number of vertex in a given graph with set of edges E, in such a way that the set contains at least one end point of every edge of the graph. It is a well known optimization problem on graphs with application in planning, development and commercial purpose. We will discuss same graph used in map coloring for this problem.

There are 7 vertices in our graph. For each vertex i we will assume a binary variable  $x_i$ . If vertex is in the cover i.e. in the subset  $x_i = 1$  otherwise  $x_i = 0$ . Then the total number of vertices in covering set can hence be written as  $\sum_{i=1}^7 x_i$  which is to be minimized.

$$\text{Total covering vertices} = \sum_{i=1}^7 x_i \quad (4.13)$$

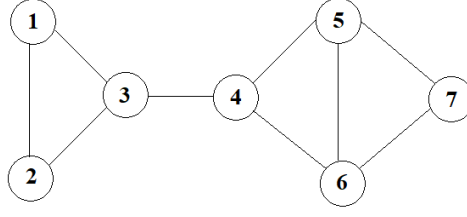


Figure 4.7: Graph for MVC problem.

$x_i$ for node i	$x_j$ for node j	Case	Penalty
0	0	both non-cover	1
0	1	one end in cover	0
1	0	one-end in cover	0
1	1	both end in cover	0

Table 4.4: Penalty formulation of Hamiltonian for MVCP.

In order to ensure that at least one of the endpoints of each edge will be in the cover, we will design a penalty function for case that violates the assumption.i.e. when both ends of edge  $ij \in E$  are not in cover, then  $x_i = 0$  and  $x_j = 0$  for which we will give a penalty 1 to increase the energy.

$$Penalty = a_i x_i + a_j x_j + b_{ij} x_i x_j + C \quad (4.14)$$

For  $x_i = 0, x_j = 0$

$$1 = a_i \cdot 0 + a_j \cdot 0 + b_{ij} \cdot 0 \cdot 0 + C \text{ gives } C = 1$$

For  $x_i = 0, x_j = 1$

$$0 = a_i \cdot 0 + a_j \cdot 1 + b_{ij} \cdot 0 \cdot 1 + 1 \text{ gives } a_j = -1$$

For  $x_i = 1, x_j = 0$

$$0 = a_i \cdot 1 + a_j \cdot 0 + b_{ij} \cdot 1 \cdot 0 + 1 \text{ gives } a_i = -1$$

For  $x_i = 1, x_j = 1$

$$0 = -1 \cdot 1 + -1 \cdot 1 + b_{ij} \cdot 1 \cdot 1 + 1 \text{ gives } b_{ij} = 1$$

Hence, we will get the equation for penalty that satisfies all cases shown in table.

$$Penalty = -(x_i + x_j) + x_i x_j + 1 \quad (4.15)$$

We will calculate total penalty for all edges  $ij \in E$  by summing above expression for each edges of set E.

$$P_{Total} = \sum_{E=ij} \left[ x_i x_j - (x_i + x_j) + 1 \right] \quad (4.16)$$

We will add equation (4.13) and equation (4.16) to get objective function which we intend to minimize



during optimization.

$$H = \sum_{i=1}^7 x_i + \sum_{E=ij} \left[ x_i x_j - (x_i + x_j) + 1 \right] \quad (4.17)$$

Then the required upper triangular matrix for given graph will be ,  $Q = \begin{pmatrix} -1 & 1 & 1 & 0 & 0 & 0 & 0 \\ 0 & -1 & 1 & 0 & 0 & 0 & 0 \\ 0 & 0 & -2 & 1 & 0 & 0 & 0 \\ 0 & 0 & 0 & -2 & 1 & 1 & 0 \\ 0 & 0 & 0 & 0 & -2 & 1 & 1 \\ 0 & 0 & 0 & 0 & 0 & -2 & 1 \\ 0 & 0 & 0 & 0 & 0 & 0 & -1 \end{pmatrix}$

so that we can write equation (4.17) in form  $H = X^T Q X + 9$  . We are in search of optimal solution  $X^* = (x_1 \ x_2 \ x_3 \ x_4 \ x_5 \ x_6 \ x_7)^T$  which minimizes Hamiltonian. The constant term 9 in our objective function can be ignored during optimization process.

# Chapter 5

## Results and Discussion

### 5.1 Simulation in 2D IM

Nine spins were put in a 3x3 square lattice with periodic boundary for simulation. Although the lattice size is very small, but it still retains features of phase transition.

#### 5.1.1 Thermalization in 2D IM

Thermalization is transition of arbitrary spin configuration towards state with uniform energy for a particular temperature. We initialize the thermalization algorithm with two types of configuration, first cold start ( all spins up ) and then hot start ( random spin configuration ), and plot the evolution of magnetization at different runs through the markov-chain. Only the thermalized samples will be considered for computation of thermodynamic quantities of interest.

The Figure 5.1 shows the thermalization for two dimensional IM with lattice size of 20X20 and 15X15 respectively at temperature  $T=6 J/K_B$  and field  $B=0$ . Black curve represents thermalization with cold start configuration whereas green curve represents thermalization with hot start configuration. The evolution of markov chain in this case settles down to zero average magnetization as shown in Figure 5.1.

The Figure 5.2 shows the thermalization at temperature  $T=5 J/K_B$  and field  $B=1$  for two dimensional lattice with lattice size of 20X20 and 15X15 respectively. In this case, the sample thermalizes at about magnetization close to 0.5. We will plot average of magnetization of such thermalized sample for discrete temperature points in plot of magnetization as a function of temperature.

We can observe the magnetization settles down after about  $1000^{th}$  run of thermalization. To be sure that the sample we are taking represents thermalized sample, we take samples  $2000^{th}$  run onwards for computation.

#### 5.1.2 Findings of 2D IM

The results of MCMC simulation in 2D Onsager lattice hence remains a brute force technique to study phase transition in non zero field. At  $B=0$ , logarithmic divergence at critical temperature has been observed ( Figure 5.3, right ) where specific heat fails to be analytic function of temperature [6].

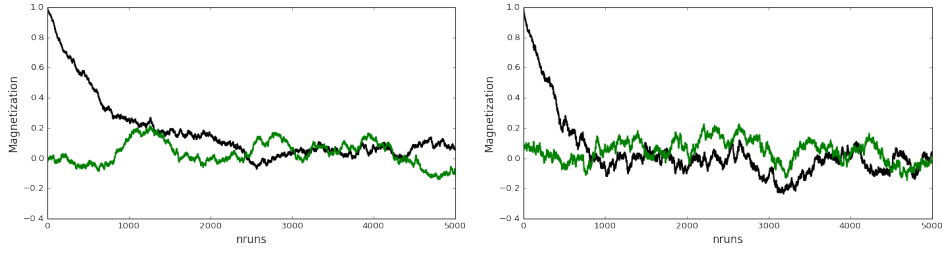


Figure 5.1: Thermalization at  $T= 6 J/K_B$ ,  $B=0$  for lattice size  $L=20$  and  $L=15$  respectively.

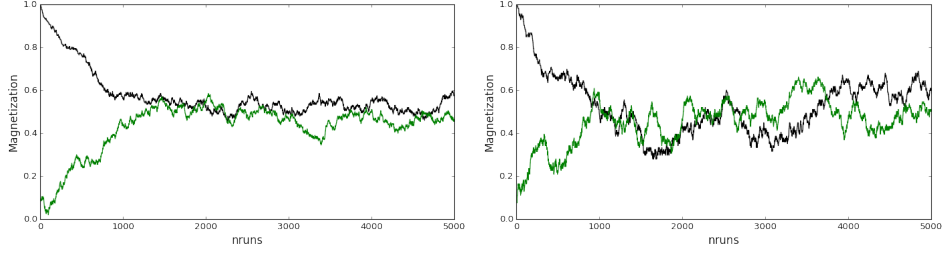


Figure 5.2: Thermalization at  $T= 5 J/K_B$ ,  $B=1$  for lattice size  $L=20$  and  $L=15$  respectively.

- A hump has been observed in specific heat of 2D IM near critical temperature for every field.
- Average magnetization shows a reflection symmetry along  $B=0$  for curves of  $\pm B$ .
- Spontaneous magnetization has been observed below  $T_c$  in absence of external field, with equal tendency to align in either +1 or -1 alignment.
- Critical temperature obtained from observation of simulation around  $T_c=2.2 J/K_B$  has been found consistent with Onsager's critical temperature of  $T_c = 2.26 J/K_B$  in Figure 5.3.
- Bifurcation below  $T_c$  in Figure 3 ( left ) shows symmetry breaking in zero field at low temperature region below  $T_c$ . Thus, doubly degenerate states of IM exist below  $T_c$ .

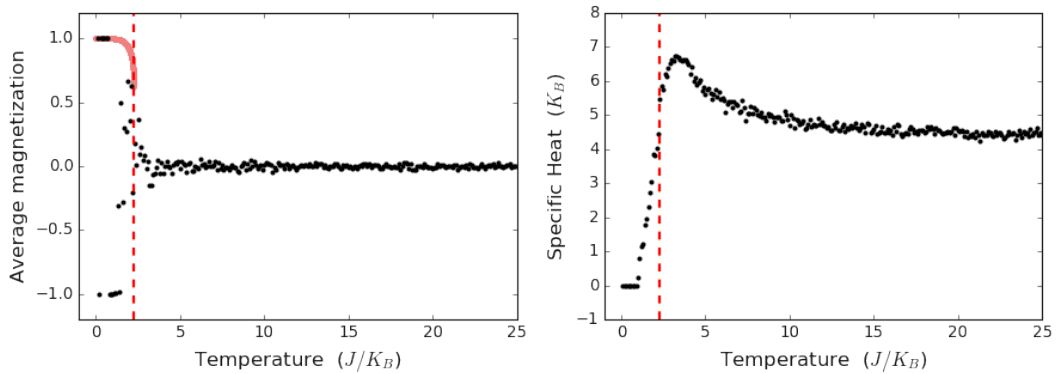


Figure 5.3: The temperature dependence of average magnetization, and specific heat at zero field. Onsager's theoritical critical point  $T_c = 2.26 J/K_B$  represented by dotted line.

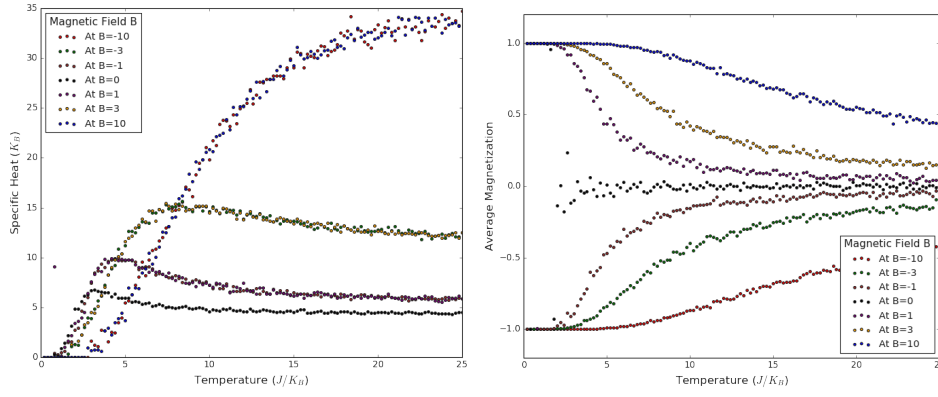


Figure 5.4: Average magnetization (upper right) and specific heat (upper left) at various fields.

## 5.2 Equivalence with Binary Variant of IM

Figure 5.5 shows simulation results with binary variant of IM, in which we assign 0s and 1s to represent spins. We discussed Hamiltonian for binary variant using penalty technique such that it retains logic of Hamiltonian for Ising Model in earlier chapter which was used for simulation with binary model.

$$H_{Ising} = -J \sum_{Edges\ i,j}^{2N} s_i s_j - \mu B \sum_{node=1}^N s_{node} \quad (5.1)$$

We can reformulate the Hamiltonian for Binary Model by starting from this transformation instead.

$$s_{binary} = \frac{1 + s_{ising}}{2}, \text{ where } s_{ising} = \pm 1 \quad (5.2)$$

Now, if we substitute  $s_{ising} = (2s_{binary} - 1)$  in eqn (5.1),

$$H_{Ising} = -J \sum_{Edges\ i,j}^{2N} (2s_i - 1)(2s_j - 1) - \mu B \sum_{node=1}^N (2s_{node} - 1) \quad (5.3)$$

On expanding equation (5.3),

$$\begin{aligned} H_{Ising} &= -J \sum_{Edges\ i,j}^{2N} [1 + 4s_i s_j - 2(s_i + s_j)] - 2\mu B \sum_{node=1}^N s_{node} + \mu B N_{nodes} \\ &= 2J \sum_{Edges\ i,j}^{2N} [(s_i + s_j - 2s_i s_j)] - 2\mu B \sum_{node=1}^N s_{node} + \mu B N_{nodes} - 2J N_{edges} \end{aligned} \quad (5.4)$$

This is identical to our formalism of Binary Hamiltonian in equation (4.5).

Comparing coefficients of equation (4.5) with equation (5.4),  $u=2J$ ,  $v=-2\mu B$

Since there appears four same indexes for every s in set of edges, we can write,

$$2J \sum_{Edges\ i,j}^{2N} [(s_i + s_j)] = 8J \sum_{node=1}^N s_i \quad (5.5)$$

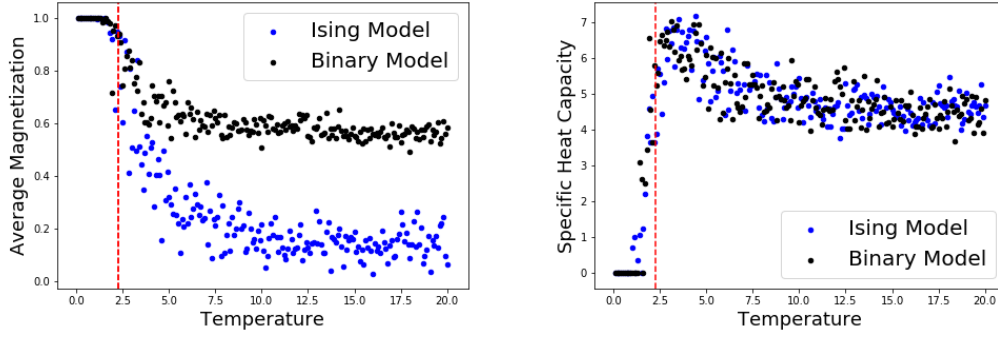


Figure 5.5: Comparison of average magnetization (upper right) and specific heat(upper left) in IM and BM at  $B=0$ ,  $T_c = 2.26 J/K_B$  represented by dotted line.

We also have, for  $N$  lattice sites in square lattice,

$$N_{nodes} = N \quad \text{and} \quad N_{edges} = 2N \quad (5.6)$$

So equation (5.4) will reduce for binary spins to

$$H_{Ising} = 2(4J - \mu B) \sum_{Nodes=1}^N s_i - 4J \sum_{Edges\ i,j}^{2N} s_i s_j + N(\mu B - 2J) \quad (5.7)$$

We will name the coefficients and use them for binary model

$$coupler(c) = -4J, \quad bias(b) = 2(4J - \mu B), \quad \text{and} \quad offset(w) = N(\mu B - 2J) \quad (5.8)$$

On averaging on both sides of  $s_{ising} = (2s_{binary} - 1)$ , we get relation of average magnetization in BM and IM given by,

$$M_{ising} = (2M_{binary} - 1) \quad (5.9)$$

We will check validity of this relation for case of  $M_{binary} = 0.6$ ,  $M_{ising}$  as predicted by equation (5.9),

$$M_{ising} = 2 \times 0.6 - 1 = 1.2 - 1 = 0.2 \quad (5.10)$$

This result is consistent with Figure 5.5 (left).

### 5.3 Simulation in 3D IM

27 spins were put in a 3X3X3 lattice with periodic boundary and thermalization was initiated with arbitrary spin configuration.

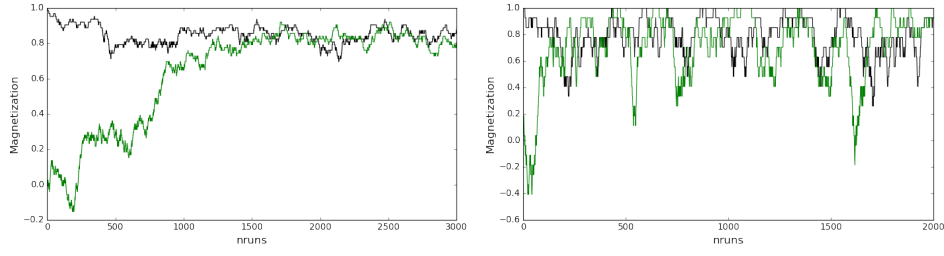


Figure 5.6: Thermalization at  $T=5 J/K_B$ ,  $B=1$  for lattice size  $L=5$  and  $L=3$  respectively in 3D IM.

### 5.3.1 Thermalization in 3D IM

Like in 2D simulation, we initialize the thermalization algorithm with cold start and hot start, and plot the evolution of magnetization at different runs through the markov chain. Only the thermalized samples will be considered for computation of thermodynamic quantities of interest.

The Figure 5.6 shows the thermalization for three dimensional lattice with lattice size of  $5 \times 5 \times 5$  and  $3 \times 3 \times 3$  respectively at temperature  $T=5 J/K_B$  and field  $B=1$ . Black curve represents initialization with cold spin configuration whereas green represents initialization with hot start configuration. We can observe the magnetization settles down at about  $1500^{th}$  thermalization in  $L=5$  and  $200^{th}$  thermalization in  $L=3$ . To be sure that the sample we are taking represents thermalized sample, we have taken samples  $2000^{th}$  nrns onwards for computation.

### 5.3.2 Findings of 3D IM:

The 3D model shows qualitatively same results as 2D. Exact solution of 3D IM doesn't exist and hence MCMC simulation is considered a powerful technique to study phase transition for higher dimensional model.

- Computational simulation suggests critical temperature around  $T_c=4.3 J/K_B$ . (Figure 5.7 )
- Simulation suggests specific heat increases linearly below  $T_c$ , falls down right after critical point and then attains nearly constant value at  $B=0$  as observed in Figure 5.7 ( right ).
- A prominent hump has been observed in specific heat of 3D IM near critical temperature for every  $B$ , showing qualitatively similar behavior as 2D.
- Average magnetization shows a reflection symmetry along line at  $B = 0$  for curves of  $\pm B$  like in 2D.
- Spontaneous magnetization has been observed below  $T_c$  in absence of external field, with equal tendency to align in either +1 or -1 alignment.
- Figure 5.9 (left) shows bifurcation below  $T_c$ . Symmetry breaking is observed in zero field at low temperature region.

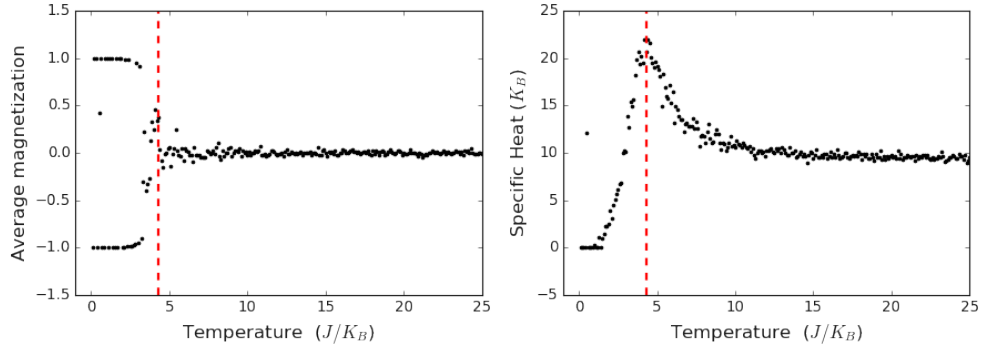


Figure 5.7: The temperature dependence of average magnetization (left) and specific heat (right) at  $B=0$ .

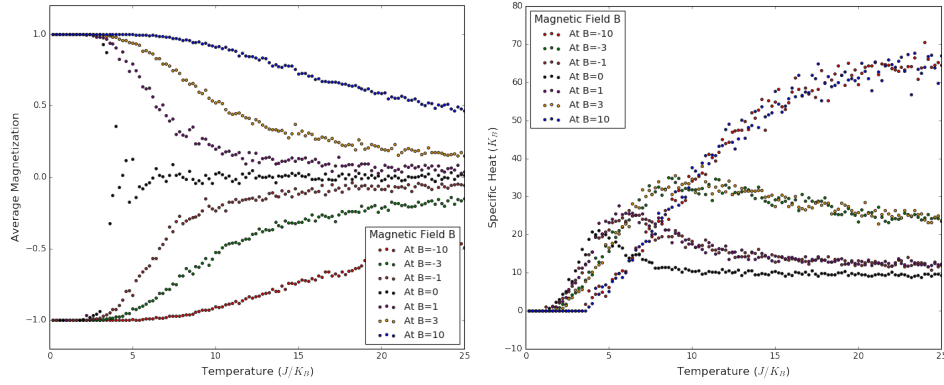


Figure 5.8: The temperature dependence of average magnetization (left) and specific heat (right) at different field in 3D IM.

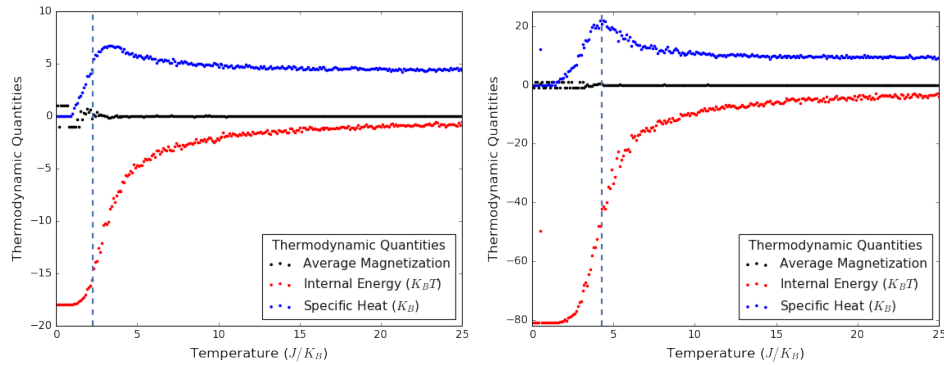


Figure 5.9: The temperature dependence of average magnetization (black), specific heat (blue) and energy (red) at zero field for 2D and 3D IM. Dotted line represents Onsager's critical point  $T_c = 2.269$  K in 2D and expected critical point in 3D.

## 5.4 Optimal Solution of QUBO Problems

### 5.4.1 Number Partitioning Problem

We got two lowest energy state  $x^* = (1 \ 0 \ 0 \ 1)^T$  and  $x^* = (0 \ 1 \ 1 \ 0)^T$  which means set  $S = \{4, 5, 7, 9\}$  is divided into two subset  $S_1 = \{4, 9\}$  and  $S_2 = \{5, 7\}$  or vice versa. The difference of sum of elements of each subsets will be 1 for this grouping which is minimum value.

### 5.4.2 Map Coloring Problem

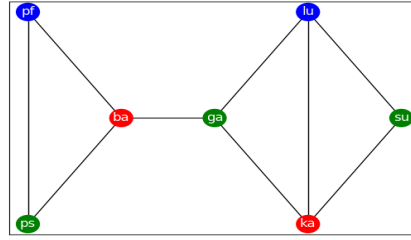


Figure 5.10: Graph solution of MCP solved using D-WAVE.



Figure 5.11: Solution of MCP, coloring seven provinces of Nepal.

Due to very large number of different combination of binary variables, it was not feasible to find the solution of this problem in classical computer and we solved this problem in D-WAVE's QPU. The solution we got was:

$$[0 \ 0 \ 1 \ 0 \ 1 \ 0 \ 1 \ 0 \ 0 \ 0 \ 1 \ 0 \ 0 \ 0 \ 1 \ 1 \ 0 \ 0 \ 0 \ 1 \ 0]^T$$

The graphical representation of this problem is shown in Figure 5.10. “pf” and “ps” denote unnamed Province-1 and Province-2 respectively, whereas first two letters of province name i.e. “ba” for Bagmati , “ga” for Gandaki , “lu” for Lumbini , “ka” for Karnali and “su” for Sudurpaschim are used in graph.



When we check the solution of map coloring problem , we find no edges having same color endpoints. This is consistent with our constraints imposed on binary variables.

In this problem , there are  $2^{21}$  possible configurations of binary variables. Classical algorithms for such optimization problems get stuck in local minimum of energy or need to go one by one through all of these states, compute their energy and find lowest energy state among them in order to reach global minimum, which consumes a lot of time, memory space and computational power.

D-WAVE QPU shows it's enormous capability of solving such optimization problems in few milliseconds. No classical computer can compute this problem as fast as quantum annealers do. The real power of annealer is when the number of binary variables in consideration are large.

### 5.4.3 Minimum Vertex Cover Problem

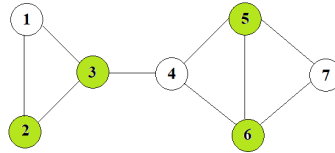


Figure 5.12: Solution-1 of MVC problem.

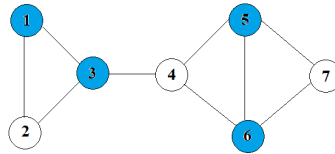


Figure 5.13: Solution-2 of MVC problem.

For MVC problem, we found 2 degenerate states satisfying our constraint in lowest energy. The optimal solutions were  $x^* = (0 \ 1 \ 1 \ 0 \ 1 \ 1 \ 0)^T$  and  $x^* = (1 \ 0 \ 1 \ 0 \ 1 \ 1 \ 0)^T$  for our graph. The solution set of minimum vertex cover are hence,  $S_1 = \{2, 3, 5, 6\}$  and  $S_2 = \{1, 3, 5, 6\}$  as shown in Figure 5.12 and Figure 5.13.

# Chapter 6

## Conclusion and Future Work

A systematic computational simulation using Markov-Chain Monte Carlo was done in finite lattice to study the behavior of critical phenomena. Simulation was done in very small lattice of size  $3 \times 3$  for both 2D and  $3 \times 3 \times 3$  for 3D.

To do this, the Metropolis algorithm was implemented in Python. Thermalization was done at constant temperature. Only thermalized samples were taken to compute average magnetization and specific heat at different external field. The dependence of temperature in average magnetization and specific heat was studied with and without external field.

### 6.1 Conclusion

The conclusions of this project work are as follows:

- The simulation of 2 D Ising Model in  $3 \times 3$  lattice exhibits phase transition at around  $T_c = 2.2 J/K_B$  as predicted by Onsager's solution. We also found critical temperature point for 3D model close to 4.3.
- Hump was observed in specific heat capacity curve in both cases of 2D lattice and 3D lattice.
- The simulation results suggest  $T_c$  at higher field will also be higher. In other words, due to the contribution of external field, there will be competition between temperature induced disorderness and biased orderness due to external B.
- The bifurcation in average magnetization curve shows symmetry breaking at zero field. This is consequence of two degenerate states of ferromagnetic model at  $B=0$ .
- Quantum annealers can be used to solve difficult combinatorial optimization problems efficiently by QUBO approach. It is faster than classical optimization algorithm.

### 6.2 Future Work

We intend to work out following tasks in the future:

- This work in 2D and 3D can be extended to models with more than two spins and with higher dimensional lattice of different topology.

- More than one spins can be flipped simultaneously and differences could be studied.
- Comparison of phase transition with greater number of spins in higher lattice size can be carried out.
- This work can be extended to calculation of observables for free fermion.
- QUBO formulation of realistic combinatorial problems could be done and used for commercial purpose.

## REFERENCES

- [1] E. Ising, *Beitrag zur Theorie des Ferromagnetismus*, Z. Physik **31**, 253 (1925).
- [2] L. Onsager, *Crystal Statistics. I. A Two-Dimensional Model with an Order-Disorder Transition*, Phys. Rev. **65**, 117 (1944).
- [3] R. P. Feynman, *Simulating Physics with Computer*, Int. J. Theor. Phys, **21**, 6 (1999).
- [4] R. B. Griffiths, *Peierls Proof of Spontaneous Magnetization in a Two-Dimensional Ising Ferromagnet*, Phys. Rev. **136**, A437 (1964).
- [5] H. A. Kramers, G. H. Wannier, *Statistics of the Two-Dimensional Ferromagnet. Part I*, Phys. Rev. **60**, 252 (1941).
- [6] B. McCoy, T. Wu, *The Two-Dimensional Ising Model*, Dover Publications (2014).
- [7] R. Feynman, *Statistical Mechanics: A Set Of Lectures*, edited by J. Shaham, CRC Press (1998).
- [8] C. Thompson, *Mathematical Statistical Mechanics*, 145, Princeton University Press (1972).
- [9] N. Metropolis, A. W. Rosenbluth, M. N. Rosenbluth, A. H. Teller, and E. Teller, *Equation of State Calculations by Fast Computing Machines*, The Journal of Chemical Physics **21**, (1953).
- [10] K. Binder, *Applications of Monte Carlo Methods to Statistical Physics*, Rep. Prog. Phys. **60**, 487 (1997).
- [11] T. D. Lee, C. N. Yang, *Statistical Theory of Equations of State and Phase Transitions. II. Lattice Gas and Ising Model*, Phys. Rev., **87**, 410 (1952).
- [12] P. L. Hammer, S. Rudeanu, *Boolean Methods in Operations Research and Related Areas*, Springer Berlin Heidelberg, Berlin, Heidelberg, **7** (1968).
- [13] E. Boros, P. L. Hammer, *The Max-Cut Problem and Quadratic 0–1 Optimization; Polyhedral Aspects, Relaxations and Bounds*, Ann Oper Res **33**, 151 (1991).
- [14] P. M. Pardalos, J. Xue, *The Maximum Clique Problem*, J Glob Optim **4**, 301 (1994).
- [15] D. Du, P. M. Pardalos, *Handbook of Combinatorial Optimization*, Kluwer Academic Publishers, Boston (1999).
- [16] G. A. Kochenberger, F. Glover, B. Alidaee, C. Rego, *A Unified Modeling and Solution Framework for Combinatorial Optimization Problems*, OR Spectrum **26**, 237 (2004).
- [17] B. Apolloni, C. Carvalho, D. de Falco, *Quantum Stochastic Optimization*, Stochastic Processes and Their Applications **33**, 233 (1989).

- [18] D. de Falco, B. Apolloni, N. Cesa-Bianchi, *A numerical implementation of quantum annealing* (1988).
- [19] A. B. Finnila, M. A. Gomez, C. Sebenik, C. Stenson, and J. D. Doll, *Quantum Annealing: A New Method for Minimizing Multidimensional Functions*, Chemical Physics Letters **219**, 343 (1994).
- [20] T. Kadowaki, H. Nishimori, *Quantum Annealing in the Transverse Ising Model*, Phys. Rev. E **58**, 5355 (1998).
- [21] S. Morita, H. Nishimori, *Mathematical Foundation of Quantum Annealing*, Journal of Mathematical Physics **49**, 125210 (2008).
- [22] F. Glover, G. Kochenberger, Y. Du, *Quantum Bridge Analytics I: A Tutorial on Formulating and Using QUBO Models*, 4OR-Q J Oper Res **17**, 335 (2019).
- [23] D-WAVE Problem-Solving Handbook-User Manual (2021).
- [24] P. Beale, R. Pathria, *Statistical Mechanics*, Academic Press (2011).
- [25] K. Huang, *Introduction to Statistical Mechanics*, John Wiley and Sons (1987).
- [26] E. Monaghan, *Phase Transitions in the Ising Model*, RHUMJ, **11**, 184 (2010).
- [27] Web<sup>1</sup>: [http://micro.stanford.edu/caiwei/me334/Chap12\\_Ising\\_Model\\_v04.pdf](http://micro.stanford.edu/caiwei/me334/Chap12_Ising_Model_v04.pdf)
- [28] M. Plischke, B. Bergersen, *Equilibrium Statistical Physics*, World Scientific, Singapore (1994).
- [29] S. Schaveling, *The Two Dimensional Ising Model*, Master Thesis, University of Ansterdam (2016).
- [30] Web<sup>2</sup>: <https://i.stack.imgur.com/g8wdG.png>
- [31] R. Landau, M. Paez, C. Bordenianu, *Computational Physics: Problem Solving with Python*, Wiley-VCH (2015).
- [32] K. Rosen, *Discrete Mathematics and Its Application*, McGraw-Hill Publication (2007).
- [33] Nielsen, Michael A and Chuang, Isaac, *Quantum Computation and Quantum information*, Cambridge University Press (2002).
- [34] C. McGeoch, *Adiabatic Quantum Computation and Quantum Annealing*, Morgan and ClayPool Publishers (2014).
- [35] D. de Falco and D. Tamascelli, *An Introduction to Quantum Annealing*, RAIRO-Theor. Inf. Appl. **45**, 99 (2011).

# **Appendix A**

## **Documentation of Codes**

All codes used in this work are organized in github repository:

[https://github.com/HariRamKrishna/Lattice\\_Models](https://github.com/HariRamKrishna/Lattice_Models)